Lecture 5: MHD Shocks and Particle Acceleration Processes

Aims, learning outcomes, and overview

Aim: To develop a detailed understanding of the physics of magnetohydrodynamic shock waves at the fluid level, and of two particle acceleration mechanisms that operate at shocks: shock drift acceleration, and diffusive shock acceleration.

Learning outcomes: At the end of this lecture, students are expected to:

- explain qualitatively what shocks are and have a basic physical understanding of them;
- explain why shocks are important in space and astrophysical plasmas;
- understand and explain qualitatively the jump conditions which represent conservation of physical quantities at shock fronts and other plasma discontinuities;
- be able to derive and use the Rankine-Hugoniot relations and jump conditions describing general magnetohydrodynamic shocks;
- understand and describe qualitatively the varieties of MHD shocks and their properties, including fast mode and slow mode shocks;
- understand the processes sometimes called "shock drift acceleration" and sometimes "magnetic mirror reflection", describe their basic physics and properties, and be able to explain them in terms of both particle motions at the shock front and reflection by a moving magnetic mirror;
- understand Fermi acceleration and be able to describe its properties and physical origin.

Overview: A *shock wave* is a disturbance that moves through a fluid faster than the characteristic speed of propagation of small amplitude waves in the medium (e.g. faster than the adiabatic sound speed in an unmagnetised plasma, or faster than the Alfvén speed in a magnetised plasma). Shocks develop because of nonlinear steepening, in which the propagation (group) speed of a wave disturbance increases with amplitude. In this case, large amplitude Fourier components of a relatively localized disturbance move faster than the small amplitude components, causing an initially Gaussian disturbance to steepen towards an almost vertical front (Figure 5.1). This nonlinear steepening then leads to either wave breaking and overturning, which lead to increased dissipation and intrinsic time variability for the disturbance, or else to increased dissipation that is large enough to balance the steepening and produce a time-stationary shock solution. The overall qualitative picture is one

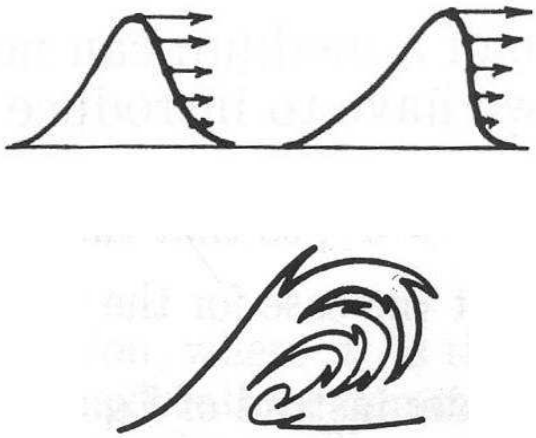

Figure 5.1: Illustrations of (Top) the nonlinear steepening of a wave into a shock and (bottom) wave breaking and overturning.

in which "excess" directed kinetic energy is redistributed into increased thermal energy and sometimes magnetic field energy.

Shocks may be produced by explosions, or when a fluid moving faster than the relevant characteristic speed encounters a slower-moving fluid, or they may be produced when a wave encounters a region where the local characteristic speed decreases in the direction of propagation of the wave. At a shock front, fluid parameters change discontinuously, because waves cannot propagate ahead to 'smooth out' the discontinuity.

Shocks are important in space physics because of their various effects, which include the heating, compression, and changed flow velocity (magnitude and direction) of the plasma plasma, the amplification (or compression) and changed direction of magnetic fields, the acceleration of small numbers of particles to high energies, and the generation of . In this lecture the theory of MHD shocks is presented, together with descriptions of two of the mechanisms whereby shocks accelerate particles – *shock drift acceleration*, and *diffusive shock acceleration*.

5.1 Jump conditions for shocks

Shock theory relates plasma properties behind the shock (referred to as downstream, subscript 2) to those ahead of the shock (upstream, subscript 1).

A boundary (an interface) between two semi-infinite plasmas with different mass densities, η, temperatures, T, and magnetic fields, $\mathbf{B}$, is illustrated in Figure 5.2. The normal to the boundary is denoted by the unit vector $\mathbf{n}$. By definition the normal points upstream perpendicular to the boundary, pointing in the $-\mathbf{x}$ direction in Figure 5.2. This boundary represents a shock in a *shock frame*, namely a frame in which the shock is at rest.

A special shock frame is the *shock normal frame* illustrated in Figure 5.2, in which the flow $\mathbf{u}_1$ is normal to the shock front. It is always possible to make a Lorentz transformation to the shock normal frame. Having found the properties of a shock in that frame, a Lorentz transformation can be made back to the frame of

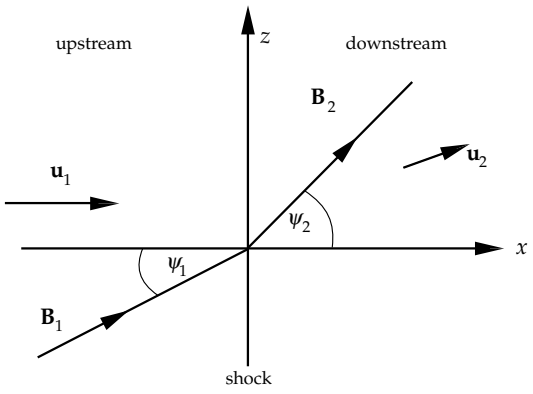

Figure 5.2: The changes in velocity and magnetic field across a shock front in the *shock normal frame*. The shock is at rest, the upstream plasma approaches with velocity $\mathbf{u}_1$ along the shock normal $\mathbf{n}$, and the downstream plasma recedes at $\mathbf{u}_2$ at an oblique angle to $\mathbf{n}$. The upstream magnetic field is at an angle ψ_1 to $\mathbf{n}$, and this changes to ψ_2 in the downstream region. Shocks with $\psi_1 = \pi/2$ are called *perpendicular* and shocks with $\psi_1 = 0$ (or $\psi_1 = \pi$) are *parallel*.

physical interest. These include the spacecraft frame, the *laboratory frame*, frames in which the Sun or Earth are at rest, etc. In general in these frames the shock is propagating obliquely from region 2 (*downstream* of the shock) into region 1 (*upstream* of the shock).

Boundary conditions that relate parameters across the interface between the two media in a shock frame are called *jump conditions*, although they are also referred to as *Rankine-Hugoniot* relations. If we denote the change in any quantity across the boundary by square brackets, then the change in a scalar quantity, A, is

$$[A] = A_1 - A_2. \tag{5.1}$$

The normal and tangential components of a vector $\mathbf{V}$ are, respectively,

$$V_n = \mathbf{V} \cdot \mathbf{n}, \qquad \mathbf{V}_t = \mathbf{V} - (\mathbf{V} \cdot \mathbf{n})\,\mathbf{n}. \tag{5.2}$$

and thus the change in V_n is

$$[V_n] = (\mathbf{V}_1 - \mathbf{V}_2) \cdot \mathbf{n}. \tag{5.3}$$

The MHD jump conditions are derived from the equations of continuity for mass, momentum and energy, together with boundary conditions arising from Maxwell's equations. The conservation law for a scalar quantity, Q, with associated flux, $\mathbf{F}$, and source term S_Q is

$$\frac{dQ}{dt} = \frac{\partial Q}{\partial t} + \nabla \cdot \mathbf{F} = S_Q. \tag{5.4}$$

If the flow creating the shock is steady then the shock is not accelerating and $\int dV\ \partial Q/\partial t = 0$ where V is an arbitrary volume. If in addition the source term is zero, then $\int dV\ dQ/dt = 0$, and the volume integral of (5.4) reduces to $\int dV\ \nabla \cdot \mathbf{F} = 0$. Converting this into a surface integral gives, for any surface S,

$$\int_S d\mathbf{S} \cdot \mathbf{F} = 0. \tag{5.5}$$

Applying this to the surface illustrated in Figure 5.3, and letting the thickness of the box shrink to zero leads to the jump condition

$$(\mathbf{F}_1 - \mathbf{F}_2) \cdot \mathbf{n} = [F_\mathrm{n}] = 0 \tag{5.6}$$

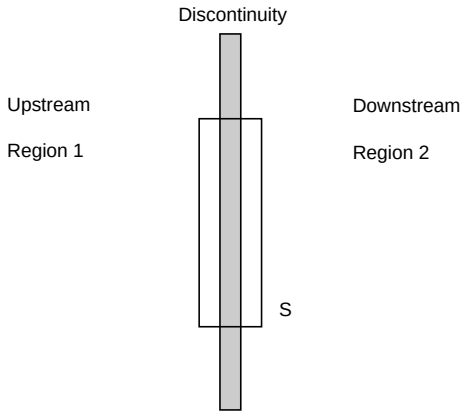

Figure 5.3: The surface S over which the integral (5.5) is performed is a box across the shock with sides parallel and normal to discontinuity.

which expresses the obvious requirement that for a conserved quantity, the incoming flux (amount per unit time, per unit area) from region 1 is equal to the outgoing flux to region 2.

For a steady flow with no source terms, the explicit form of (5.4) for mass conservation ($Q \to \eta$ = mass density, $\mathbf{F} \to \eta\mathbf{u}$, $\mathbf{u}$ = flow velocity) is

$$\nabla \cdot (\eta \mathbf{u}) = 0 \ , \tag{5.7}$$

and so the jump condition that expresses mass conservation is, from (5.6) and (5.7),

$$[\eta u_n] = 0 \ . \tag{5.8}$$

The corresponding form of (5.4) for energy is

$$\nabla \cdot \left(\frac{1}{2}\eta u^2 \mathbf{u} + \frac{\Gamma P}{\Gamma - 1}\mathbf{u} + \frac{\mathbf{E} \times \mathbf{B}}{\mu_0} \right) = 0, \tag{5.9}$$

where the first term describes the kinetic energy flux, the second is the flux of thermal energy (the enthalpy flux) with Γ the ratio of the specific heats, and the final term is the electromagnetic energy flux (the Poynting vector). The jump condition related to energy conservation follows by eliminating $\mathbf{E}$ from (5.9) by assuming that the plasma is infinitely conducting so that $\mathbf{E} = -\mathbf{u} \times \mathbf{B}$. The Poynting vector is then given by $\mathbf{E} \times \mathbf{B}/\mu_0 = (B^2\mathbf{u} - \mathbf{u} \cdot \mathbf{B}\,\mathbf{B})/\mu_0$, and it follows that

$$\left[\frac{1}{2}\eta u^2 u_n + \frac{\Gamma}{\Gamma - 1} P u_n + \frac{B^2}{\mu_0}\, u_n - \frac{\mathbf{u} \cdot \mathbf{B}}{\mu_0} B_n \right] = 0. \tag{5.10}$$

The conservation equation for momentum is more complicated because the momentum density $\eta\mathbf{u}$ is a vector, and the counterpart of the flux is the stress tensor, $\mathbf{S}$. Denoting the ij-component of the stress tensor by $\mathrm{S}_{ij} (= \mathrm{S}_{ji})$,

$$\mathrm{S}_{ij} = \eta u_i u_j + P\delta_{ij} + \left(\frac{\varepsilon_0 E^2}{2} + \frac{B^2}{2\mu_0} \right) \delta_{ij} - \varepsilon_0 E_i E_j - \frac{1}{\mu_0} B_i B_j. \tag{5.11}$$

The first term in (5.11) describes the stress due to the bulk motion, the second is the isotropic pressure resulting from random thermal motions, the next two terms are the electric and magnetic pressures, and the final terms describe the stresses associated with the tensions along the electric and magnetic field lines. The counterpart of (5.8) or (5.9) for the ith component of the momentum flux is of the form $\partial \mathrm{S}_{ij}/\partial x_j = 0$ (where a sum over $j = x,\ y,\ z$ is implied). The quantity $\mathbf{S} \cdot \mathbf{n}$ is

a vector with normal and tangential components. These components give jump conditions expressing conservation of the normal and tangential components of the momentum flux, respectively (terms involving the electric field are neglected):

$$\left[\eta u_n^2 + P + \frac{B_t^2}{2\mu_0}\right] = 0, \tag{5.12}$$

and

$$\left[\eta u_n \mathbf{u}_t - \frac{B_n}{\mu_0}\mathbf{B}_t\right] = 0. \tag{5.13}$$

The quantity $P_{ram} = \eta u_n^2$ will be called the *ram pressure below*. It is vital in understanding the qualitative physics and location of shocks and other related discontinuities.

In addition to the jump conditions (5.8), (5.10), (5.12) and (5.13), Maxwell's equations also require that the normal component of $\mathbf{B}$ and the tangential component of $\mathbf{E}$ are continuous. The first of these conditions may be written

$$[B_n] = 0. \tag{5.14}$$

The continuity of the tangential component of $\mathbf{E}$ is equivalent to the continuity of

$$\mathbf{n} \times \mathbf{E} = (\mathbf{u} \times \mathbf{B}) \times \mathbf{n} = \mathbf{u} \cdot \mathbf{n}\,\mathbf{B} - \mathbf{B} \cdot \mathbf{n}\,\mathbf{u},$$

which implies

$$[u_n \mathbf{B}_t - B_n \mathbf{u}_t] = 0. \tag{5.15}$$

We now combine (5.8), (5.10), and (5.12)–(5.15) into a single equation. that can be solved and used to describe the properties of shocks and related discontinuities.

5.2 Magnetohydrodynamic Shocks

The first step is to choose the shock normal frame, in which $u_1 = u_{1n}$. It is also convenient to introduce the Alfvén Mach number:

$$M_A := \frac{u_1}{v_{1A}}, \qquad \text{where} \qquad v_{1A}^2 := \frac{B_1^2}{\mu_0 \eta_1}. \tag{5.16}$$

The Mach number and the angle θ between the shock normal direction and the upstream magnetic field ($\theta = \psi_1$ in Figure 5.1) are the two independent parameters that define a magnetized shock. We also introduce the compression ratio, $r := \eta_2/\eta_1$ and note that the jump condition (5.8) implies

$$\eta_1 u_{1n} = \eta_2 u_{2n} \quad \text{or} \quad r = \frac{\eta_2}{\eta_1} = \frac{u_{1n}}{u_{2n}}. \tag{5.17}$$

The motivation is to eliminate all the variables relating to the downstream region. The normal component of the magnetic field in the downstream region is removed using the jump condition (5.14), which implies that $B_{2n} = B_{1n}$. Then $\mathbf{u}_{2t}$ may be eliminated between jump conditions (5.13) and (5.15), leading to

$$\mathbf{B}_{2t} = \mathbf{B}_{1t} \frac{r(M_A^2 - \cos^2\theta)}{M_A^2 - r\cos^2\theta}. \tag{5.18}$$

and

$$\mathbf{u}_{2t} = \mathbf{B}_{1t} \frac{u_1(r-1)\cos\theta}{B_1(M_A^2 - \cos^2\theta)}. \tag{5.19}$$

Finally, eliminating P_2 between jump conditions (5.10) and (5.12) and using equations (5.18) and (5.19) leads to the equation for the Alfvén Mach number

$$\left(\frac{aM_A^2}{r}-\beta\right)\left(\frac{M_A^2}{r}-\cos^2\theta\right)^2-\frac{M_A^2}{r}\sin^2\theta\left[\frac{M_A^2}{r}\left(a+\frac{r-1}{2}\right)-a\cos^2\theta\right]=0, \tag{5.20}$$

where $\beta := c_{1s}^2/v_{1A}^2$, with $c_{1s}=(\Gamma P_1/\eta_1)^{1/2}$, and where $2a=\Gamma+1-r(\Gamma-1)$.

Equation (5.20) has a variety of solutions, each of which describes a discontinuous transition, but not all of which are shocks. The description "shock" is usually restricted to compressive discontinuities (i.e. those for which $r=\eta_2/\eta_1>1$). This restriction is physically motivated: it may be shown that entropy increases at the discontinuity only for $r>1$. Hence rarefactional shocks do not exist. In the following discussion we focus on solutions to equation (5.20) of relevance to space physics.

First note that (5.20) is a cubic in M_A^2, and so in general it has three solutions. In the limit of a weak discontinuity, i.e. for $r\to 1$, $a\to 1$, (5.20) reduces to the dispersion equation for the three MHD wave modes, viz. the Alfvén mode, and the fast and slow magnetoacoustic modes, as discussed in Lecture 2.

Second, accordingly, the solutions of (5.20) are classified according to the related MHD modes, that is, as fast mode or slow mode shocks. The counterpart of Alfvén waves is not normally considered to be a shock because, like small amplitude Alfvén waves, it does not compress the plasma – in general the Alfvén mode corresponds to a *tangential discontinuity*, or *rotational discontinuity*, at which the transverse component of the magnetic field reverses direction. The solution in this case is $r=1$, $M_A^2=\cos^2\theta$. A phenomenological distinction between fast and slow mode shocks is that the magnetic field increases in a fast mode shock, and decreases or stays the same in a slow mode shock.

Third, shocks involve a finite compression of the plasma, a property that can be demonstrated by dividing equation (5.20) by $(M_A^2)^3$ and taking the limit $M_A\to\infty$. This leads to the requirement $r\to(\Gamma+1)/(\Gamma-1)$. Hence the density ratio r cannot be arbitrarily large; for $\Gamma=5/3$ the limiting value is $r=4$, so that no shock can lead to a compression in density greater than a factor of four (provided $\Gamma=5/3$). By reference to equation (5.18) it is clear that the increase in the magnetic field at a strong shock is also limited to a factor of four.

Fourth, the Rankine-Hugoniot analysis above is based only on conservation of mass, momentum, energy, and electromagnetic field quantities on either side of a suitably narrow discontinuity and with suitable time and volume averaging. It does not address the detailed structure of the transition layer, but only the properties of the upstream and downstream plasma suitably far from the transition. Accordingly, significantly larger compressions in density and magnetic field strength are possible in the immediate vicinity of the shock, as discussed in later lectures. Moreover, the jump conditions apply also to other types of boundaries, including planetary magnetopauses and both rotational and tangential discontinuities.

For parallel propagation ($\theta=0$), (5.20) has solutions

$$M_A^2=r, \qquad M_A^2=r\beta/a, \tag{5.21}$$

with $M_A^2=r$ being a double solution. The solution $M_A^2=r\beta/a$ is an example of a slow mode shock. This solution may be written $(u_1/c_{1s})^2=r/a$ and corresponds to an unmagnetized shock solution (the same solution is obtained from the jump conditions with $\mathbf{B}=0$). In this case the magnetic field does not change across the front, and so does not participate in the shock process. The other solution ($M_A^2=r$) is a fast mode shock. In this case neither $\mathbf{u}_2$ nor $\mathbf{B}_2$ is along $\mathbf{n}$, and the solution is called a *switch-on shock* because the tangential component of $\mathbf{B}$ switches on as the front passes.

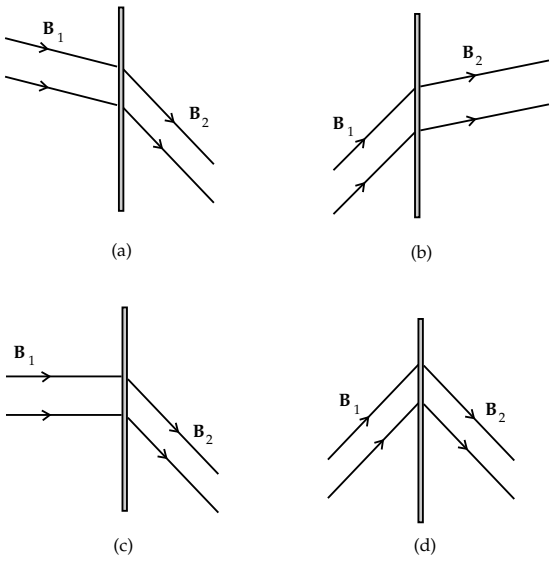

Figure 5.4: Discontinuities in a magnetized plasma: (a) a fast mode shock, (b) a slow mode shock, (c) a switch-on shock, and (d) a tangential discontinuity (an Alfvénic shock).

For perpendicular propagation ($\theta = \pi/2$), (5.20) has the solution

$$M_A^2 = (r/a)\left[\beta + 1 + (r-1)(1-\Gamma/2)\right]. \tag{5.22}$$

In this case $B_{2t}/B_{1t} = B_2/B_1 = r$, and since the magnetic field increases, this is a fast mode shock. There is no perpendicular slow mode shock, which might be expected because (small amplitude) slow mode waves do not propagate perpendicular to the magnetic field (Lecture 2).

The various phenomenological cases are illustrated in Figure 5.4.

5.3 Qualitative shock physics and properties

The requirement that $r > 1$ for a shock mean immediately from Eq. (5.8) that $U_{2n} < u_{1n}$, so that the flow is slowed (in the shock normal frame) downstream of the shock. From Eqs (5.18) and (5.19) it is clear that $\mathbf{u}_{2t} \neq 0$ and $\mathbf{B}_{2t} \neq 0$ in general. Thus shocks tend to slow and deflect the incoming flow, in shock normal frame.

Turning to Eq. (5.12), taking a factor of $\eta_1 u_{1n}^2$ outside of the upstream term it can be seen that the pressure and magnetic terms have characteristic size M_S^{-2} and M_A^{-2}, respectively. When $M_A, M_S \gg 1$ the ram pressure term $P_{ram} = \eta_1 u_{1n}^2$ dominates the upstream momentum. On the downstream side, however, the term $\eta_2 u_{2n}^2 = P_{ram}/r$ so that the thermal pressure and magnetic terms must dominate. Typically the thermal pressure terms dominate. Qualitatively, then, stationary shocks can be understood in terms of a balance between the upstream ram pressure and the downstream thermal pressure. Furthermore, normal momentum balance allows us to estimate the amount of downstream heating required for a stationary solution:

$$P_2 = \eta_2 k_B T_2 = P_{ram} = \eta_1 u_{1n}^2 \,. \tag{5.23}$$

Typically the amount of heating required is large. This conclusion is robust since it is essentially based only on conservation of mass, momentum, energy, and field quantities. Put another way, the shock system must adapt until it finds a heating mechanism able to satisfy the conservation laws or else must be intrinsically time-variable and non-stationary.

Turning to Eq. (5.18) for fast mode shocks in the limit $M_A^2 \gg r\cos^2\theta$ it is easy to see that the M_A^2 terms dominate the numerator and denominator, but cancel so that $B_{2t} \approx rB_{1t}$. With $B_{1n} = B_{2n}$ from Eq. (5.14) it is now clear that both B and η are amplified by the same approximate factor of r.

Characteristically, then, fast mode shocks tend to slow, deflect, compress, and heat the incoming plasma, as well as amplifying and rotating the magnetic field. These characteristics lead to significant acceleration and heating of plasma particles, as described next.

5.4 Shock drift acceleration and magnetic mirror reflection

Shock drift acceleration and magnetic mirror reflection both involve the energization of particles by shock fronts due to the particles undergoing ∇B (and curvature) drifts parallel to $q\mathbf{E}_{con}$, where $\mathbf{E}_{con}$ is the convection electric field in the upstream (and downstream) plasma. These particles can be reflected by or transmitted from the shock's magnetic gradient, with the largest energy gains occurring for reflected particles. Historically the former term was applied primarily to particles with large gyroradii, which saw the shock as an abrupt transition, while the latter was applied primarily to particles with small gyroradii for which adiabatic motions characteristic of orbit theory apply.

Shock drift acceleration and magnetic mirror reflection occur at a shock front when a particle is reflected or transmitted by the front. A number of conditions need to be met for the process to be an efficient acceleration mechanism. First, the speed of the particle needs to be larger than the speed of the shock relative to the upstream plasma, so that a particle undergoes many orbits as it passes the front. Second, the largest energies are achieved at shock fronts that are nearly perpendicular (i.e. $\psi_1 \approx \pi/2$ in Figure 5.2).

The basic mechanism may be understood from Figure 1.5 of Lecture 1 and Figure 5.5 of this Lecture. Figure 5.5(a) shows a perpendicular shock viewed in the shock normal frame (the shock surface lies in the x-y plane). Figure 5.4(b) illustrates the same shock viewed along the x-axis, together with the orbit of an electron crossing the shock. Because the magnetic fields (and hence the gyroradii) are different on the two sides of the shock, there is a gradient in the magnetic field and so the particle undergoes a ∇B drift along the shock front (see Lecture 1), as illustrated in the figure. There is an identical electric field on both sides of the shock front, actually the standard convection electric field associated with the frozen-in magnetic field, given by

$$\mathbf{E} = -\mathbf{u}_1 \times \mathbf{B}_1 = -\mathbf{u}_2 \times \mathbf{B}_2. \tag{5.24}$$

This electric field accelerates the electron during its motion on the large circle (in the upstream region) and decelerates the electron during its motion on the small circle (downstream). However, the particle spends more time moving along the large circle than it does along the small circle, and so it gains energy during the drift along the shock front. Put another way, the particle gyrocenter has $q\mathbf{v}_d.\mathbf{E} > 0$, where v_d is the ∇B drift velocity given by Eq. (1.25), so that there is a continual net positive acceleration. Note that in this case there is zero curvature drift.

In the more general case of an oblique fast mode shock both the ∇B and curvature drifts can contribute, often competing. Which one dominates the energy gain then depends of the magnetic field gradient, curvature, and the values of $v_\perp$ and $v_\parallel$ for the incident particle.

Shock drift acceleration and magnetic mirror reflection result in relatively modest increases in particle energies. Quantitative treatments of the theory show that

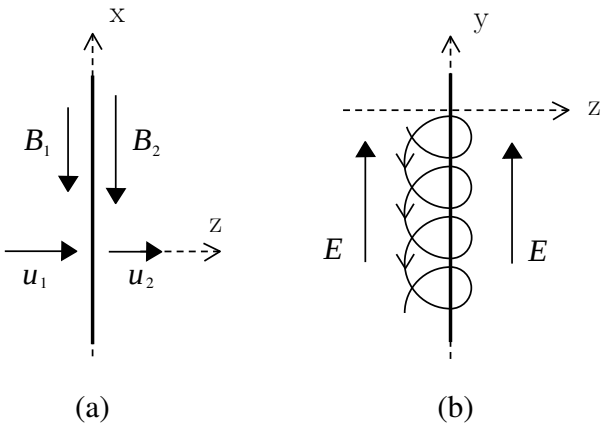

Figure 5.5: (a) A perpendicular shock in the normal incidence frame. (b) The orbit of an electron crossing the shock.

the increase is at most a factor of approximately 10 for a single encounter with the shock. However, larger gains are possible if the particles encounter the shock multiple times, due to either some scattering process or due to the combination of shock curvature and upstream magnetic field curvature.

This process can also be treated directly in terms of reflection of a particle by the shock's moving *magnetic mirror*, providing an alternative way to think about shock drift acceleration. An analogy with hitting a ping-pong ball is helpful, immediately telling us that a more rapidly moving reflected particle results from either a faster moving ping-pong bat or a particle with larger initial velocity directed towards the shock (larger relative velocity).

A particle encountering a shock may either be reflected or transmitted at the shock, and in both cases the shock drift mechanism operates to increase the energy of the particle. A condition for reflection of a particle may be obtained as follows. First, it turns out that the magnetic moment of the particle, which can be written as $p^2 \sin^2\alpha/B$ where α is the pitch angle, is almost conserved (in an average over gyrophase) when a particle crosses a shock front, so that

$$\frac{p_2^2 \sin^2\alpha_2}{B_2} = \frac{p_1^2 \sin^2\alpha_1}{B_1}. \tag{5.25}$$

Remarkably this is true not just for particles with Larmor radii $r_l \ll L$, the shock thickness, which we expect from adiabatic theory, but also for particles with $r_l \gg L$.

For a quasi-perpendicular shock there is a special shock frame, called the *de Hoffmann–Teller* frame (dHT), in which the convection electric field vanishes (and the points of intersection of field lines and the shock front are at rest). In the dHT frame the fluid velocity is parallel to the field lines on both sides of the shock (if this were not so, the plasma motion perpendicular to the field lines would imply a motion of the magnetic field at the shock front, since the field is frozen in to the plasma). According to Eq. (5.24) there is no electric field in the dHT frame, and so the energy (and hence the magnitude of the momentum) of the particle is conserved. (More accurate non-MHD theory shows that a cross-shock potential exists; this effect can be included easily but is ignored here.) Denoting quantities in the dHT frame by primes, we have $|p_1'| = |p_2'|$, and hence from equation (5.25), $\sin^2\alpha_2' = (B_2'/B_1')\sin^2\alpha_1'$. Particles with $\sin^2\alpha_1' > B_1'/B_2'$ would have pitch angles such that $\sin^2\alpha_2' > 1$ if they were transmitted through the shock. This is of course impossible, and so these particles are reflected rather than transmitted. Hence the condition for reflection is

$$\sin\alpha_1' > (B_1'/B_2')^{1/2}. \tag{5.26}$$

This type of magnetic bottle condition was discussed in Lecture 1. Eqs (1.41) and (1.42) apply also, and can be generalized easily to include the cross-shock potential. As in Lecture 1 it also follows that the reflected particles have a loss-cone distribution, while the transmitted particles are those that lie in the shock's loss cone. Thus, both the reflected and transmitted particles will have distribution functions that are significantly modified by the magnetic mirror, with gradients in velocity space that are conducive to wave growth.

Consider a reflected particle, with a velocity before reflection denoted by the subscript i, and a velocity after denoted by f. Transforming the parallel velocity of the particle from the dHT frame back to the frame of the upstream plasma gives (in the nonrelativistic approximation)

$$v_i^{\parallel} = v_i^{\parallel\prime} - u_1', \qquad v_f^{\parallel} = v_f^{\parallel\prime} - u_1'. \tag{5.27}$$

By the choice of the dHT frame we have $v_i^{\parallel\prime} = -v_f^{\parallel\prime}$. From these equations

$$\begin{aligned} v_f^{\parallel} &= -v_i^{\parallel\prime} - u_1' \\ &= -v_i^{\parallel} - 2u_1'. \end{aligned} \tag{5.28}$$

Also, the velocity of the shock in the normal direction is $u = -u_1' \cos\psi_1'$, and noting that the magnetic field does not change between frames in nonrelativistic transformations (so that the angle of the magnetic field is unchanged) we have

$$v_f^{\parallel} = 2u \sec\psi_1 - v_i^{\parallel}. \tag{5.29}$$

The speed $u\sec\psi_1$ is the speed of the dHT frame along the shock surface. Equation (5.27) demonstrates that larger energy increases (for reflected particles) occur for shocks that are more nearly perpendicular and/or moving faster relative to the upstream plasma. This recovers the result expected from the ping-pong bat analogy.

Note that for exactly perpendicular shocks the dHT speed exceeds the speed of light, so there is no dHT frame and a different approach must be used. In this cases there are no reflected particles, though, and all incident particles are transmitted through the shock. This can be seen directly from Figure 5.5, because $\mathbf{u}_1$ equals the $\mathbf{E}\times\mathbf{B}$ velocity and $\mathbf{B}$ is along the shock surface so that all particle gyrocenter velocities are necessarily directed downstream.

The strongest evidence for shock drift acceleration and magnetic mirror reflection comes from observations of shocks in the heliosphere, in particular the Earth's bow shock and interplanetary shocks. These cases will be treated in detail in later lectures (Lectures 10-14).

5.4 Diffusive shock acceleration

Diffusive shock acceleration is an example of a mechanism first recognised by Fermi in 1949 and now called the Fermi mechanism. The specific problem discussed by Fermi was the acceleration of cosmic rays via collisions with magnetized interstellar clouds. The magnetic field of a moving cloud can reflect (or scatter) a cosmic ray, as illustrated in Figure 5.6. A particle reflected from an approaching surface gains energy, and a particle reflected from a receding surface loses energy, just as for a ping-pong bat, so in general the particle's energy changes as a result of the reflection.

This process can be treated quantitatively by noting that there is no energy change in a frame in which the reflecting surface is at rest. Let u denote the velocity of the reflecting surface in the observer's frame, v_1 and v_2 denote the particle's velocity before and after reflection, and indicate velocities measured in the

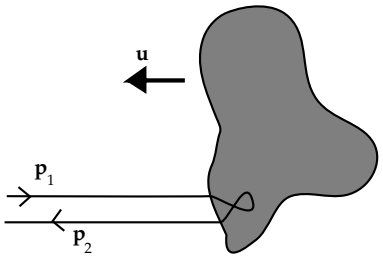

Figure 5.6: Fermi acceleration: a cosmic ray is reflected by an approaching magnetised cloud (shaded region).

rest frame of the reflecting surface by primes. Assuming all motions are collinear for simplicity, and restricting ourselves to the non-relativistic case (the relativistic generalisation is straightforward), we have

$$v_1' = v_1 - u, \qquad v_2' = v_2 - u \ . \tag{5.30}$$

In the rest frame of the reflecting surface, the particle does not gain energy in reflection and so $v_2' = -v_1'$. Equations (5.30) then give $v_2 = 2u - v_1$, analogously to magnetic mirror reflection in the previous section, and hence the observed change in energy of the particle is

$$\Delta\varepsilon = \frac{1}{2}m(v_2^2 - v_1^2) = 2m(u^2 - v_1 u). \tag{5.31}$$

As stated above, energy gains result from head on collisions ($v_1 u < 0$) and energy losses result from overtaking collisions ($v_1 u > u^2$). When energy changes are averaged over large numbers of collisions, the terms which are first order (in u) sum to zero. However, the second order changes, due to the term $2mu^2$ in (5.31), do not average to zero and so a acceleration of the particle results. This process is now often referred to as *second-order Fermi acceleration*.

In a subsequent paper in 1953. Fermi pointed out that the acceleration can be much more efficient if it is first order, and that first order changes need not always cancel. A simple example is when reflecting surfaces approach each other. A particle bouncing back and forth between approaching surfaces is always reflected head on and so the first order changes in energy are always positive. Processes of this type are called *first-order Fermi acceleration*.

First-order Fermi acceleration occurs naturally at any shock front, a process called diffusive shock acceleration, provided only that fast particles are scattered on either side of the shock. The only important point needed to understand this process is that the fluid velocity changes across the shock. Imagine a fast particle, with speed $v \gg u_1$, in the upstream plasma about to cross the shock and enter the downstream plasma. Recall the general shock configuration shown in Figure 5.2. For simplicity we consider a simple case in which $\mathbf{u}_1$ and $\mathbf{u}_2$ are normal to the shock. MHD waves can efficiently scatter fast particles, and these waves are convected along with the plasma. MHD waves in the downstream plasma are therefore moving at the fluid velocity $\mathbf{u}_2$, and so these centers are approaching with velocity $-(\mathbf{u}_2 - \mathbf{u}_1)$ with respect to the upstream plasma, as shown in Figure 5.7(a). When the particle enters the downstream plasma and is scattered, its energy is increased because the reflection is head on. In effect the scattering centers act like particles with infinite mass, so that the reflection is analogous to that from a moving wall. Now consider a particle in the downstream plasma about to cross the shock and enter the upstream plasma. As viewed from the downstream plasma, the upstream plasma is approaching with velocity $\mathbf{u}_1 - \mathbf{u}_2$, and the shock is receding with velocity -$\mathbf{u}_2$,

as illustrated in Figure 5.7(b). The scattering centers in the upstream plasma are again approaching the particle. As before, when the particle crosses the shock and is scattered, the scattering is head on and so causes an increase in the particle energy.

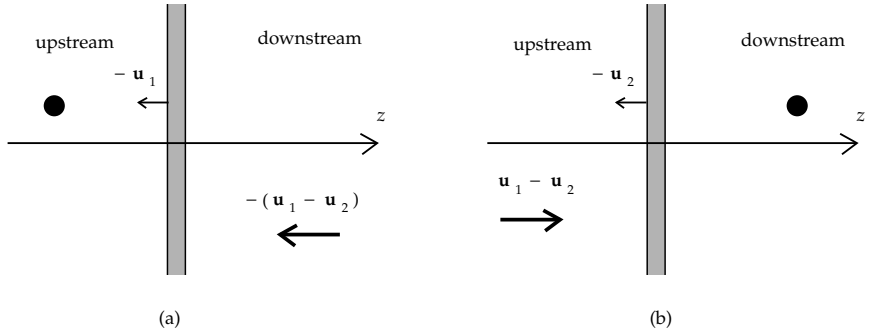

Figure 5.7: (a) A particle, denoted by the black circle, at rest in the upstream plasma sees both the shock, and (more slowly) the downstream plasma behind the shock, approaching it. (b): As for (a) but for a particle at rest in the downstream plasma which again sees the plasma on the other side of the shock approaching, but sees the shock receding.

Fermi also gave a simple argument that the first-order process leads to a power-law distribution for the energies of accelerated particles, as follows. The energy change from one head-on reflection, according to (5.31) is $\Delta\varepsilon = 2m|v_1 u|$, where we have assumed that the speed of the particle is much greater than the speed of the obstacle, and so have neglected the first term in (5.31). Now consider subsequent reflections from approaching obstacles, separated by a distance L. For $|u| \ll |v_1|$, we can consider L to be almost constant. The time between collisions is then $\Delta t = L/|v_1|$, and dividing $\Delta\varepsilon$ by Δt gives the rate of gain of energy of the particle, $d\varepsilon/dt = 2m|u|v_1^2/L = 4(|u|/L)\varepsilon$. Hence the energy of the particle after a time t is

$$\varepsilon = \varepsilon_0 \exp(\alpha t), \tag{5.32}$$

where $\alpha = 4|u|/L$. Now consider how the particle escapes from the system. A reasonable assumption is that the particle has a constant probability of escaping per unit time, described by a mean loss rate λ. In that case the probability distribution for the particle lasting a time t is the Poisson interval distribution,

$$\text{prob}(t) = \lambda e^{-\lambda t} \tag{5.33}$$

[$\text{prob}(t)\,dt$ is the probability that a particle lasts a time t in the system]. The probability distribution function for the energy of the particle, $\text{prob}(\varepsilon)$ is obtained by changing variables: $\text{prob}(\varepsilon)d\varepsilon = \text{prob}(t)\,|dt/d\varepsilon|\,d\varepsilon$. Using (5.32) and (5.33) leads to $\text{prob}(\varepsilon) \sim \varepsilon^{-(1+\lambda/\alpha)}$.

Provided that particles cross the shock many times, this mechanism allows efficient acceleration. Moreover, fast particles are expected to cross the shock many times if they are efficiently scattered on each side of the shock. This is because scattering causes spatial diffusion, so that the motion of a typical scattered particle has a random component that gives it a high probability of returning to the shock many times. Collectively, particles diffuse away from the shock. Particles wandering upstream reach a steady state with those wandering back to the shock, and the upstream particle distribution falls off with distance from the shock, approaching zero far from the shock. Particles wandering downstream can reach arbitrarily far downstream and never return, so that the downstream distribution approaches a constant arbitrarily far away from the shock.

A quantitative treatment of diffusive shock acceleration predicts that, given a mono-energetic spectrum of injected particles, the downstream spectrum of accelerated particles follows a power law form $f(p) \propto p^{-b}$, where the power-law index b depends only on the compression ratio of the shock: $b = 3r/(r-1)$. This result is consistent with observed cosmic ray energy spectra.

References

This lecture is based on a lecture by M. Wheatland, itself based on an outline of mine and earlier lectures by D.B. Melrose and L.T. Ball. In addition the following references were used.

Huba, J.D. 2006, *NRL Plasma Formulary*, Naval Research Laboratory, Washington DC (may be ordered for free from http://wwwppd.nrl.navy.mil/nrlformulary/)

Melrose, D.B. 1986, *Instabilities in Space and Laboratory Plasmas*, Cambridge University Press, Cambridge, pp. 23.-250

Thompson, W.B. 1962, *An Introduction to Plasma Physics*, Addison-Wesley, Reading, Massachusetts, pp. 86–95

Toptyghin, I.N. 1980, Space Science Reviews, **26**, 157–213

Yuan, X., I.H. Cairns and P.A. Robinson, Numerical simulation of electron distributions upstream and downstream of high Mach number quasiperpendicular collisionless shocks, J. Geophys. Res., **113**, A08109, 2008.